Characterization of Local Order in Atactic Polystyrene Using Two-Dimensional Nuclear Magnetic Resonance and Atomistic Simulations

P. Robyr,[†] M. Tomaselli,[‡] C. Grob-Pisano,[‡,§] B. H. Meier,[†,||] R. R. Ernst,[†] and U. W. Suter*[,‡]

Laboratorium für Physikalische Chemie and Institut für Polymere, Eidgenössische Technische Hochschule, CH-8092 Zürich, Switzerland

Received January 30, 1995[⊗]

ABSTRACT: The local ordering of the phenyl groups in amorphous atactic polystyrene is investigated by radio-frequency-driven carbon-13 NMR polarization transfer (spin diffusion) between site-selectively carbon-13 labeled monomer units. The NMR data agree with atomistic simulations of atactic amorphous polystyrene where orientational correlations among the phenyl rings do not extend over distances larger than 5 Å. This finding is at variance with earlier X-ray and neutron diffraction measurements.

1. Introduction

Amorphous materials lack long-range order. However, short-range order is possible. The detection and the quantification of short-range order in amorphous polymers are not yet satisfactorily solved. The difficulties root in the experimental techniques and in the reduction of the experimental data. Wide-angle diffraction, generally used for these investigations, samples the interactions between all scattering centers. When studying local order in polymers, it is necessary to separate the order between from the correlations within the monomer units during the data analysis.[1−4] The models used to compute scattering functions for comparison with the corrected experimental data range from rotational isomeric state (RIS) representations of single chains[1,2] to the concept of paracrystallinity.[3] These models include intrinsic order in terms of a restricted number of chain conformations or in terms of frustrated "microcrystallites". They might be inadequate to describe amorphous solids.

Nuclear magnetic resonance (NMR) has been recently used, in combination with calculations of isotropic chemical shifts, to study the conformational statistics in bulk polyisobutylene.[5] The method is based on the influence of local conformation on the chemical shielding. It is, however, limited to systems with large conformation-dependent chemical shift effects.

We present an alternative approach for quantifying local order in polymers, based on two-dimensional (2D) radio-frequency-driven polarization-transfer NMR spectroscopy[6−8] that has the potential to investigate the polymer chain conformation and the packing between different chains. We give a comparison of the experimental results with detailed atomistic simulations of an amorphous polymer.[9] This approach uses the sensitivity of the NMR resonance frequencies to the orientation of a structural subunit in the static magnetic field and the strong dependence of the polarization-transfer rate on the distances between the spins involved. Measuring polarization-transfer rate constants between groups of spins that resonate at different frequencies provides information about the mutual orientation of subunits in spatial proximity. To demonstrate the possibility of extracting information on the short-range order in amorphous polymer solids, we chose atactic polystyrene (a-PS), since recent experimental evidence[1−4] seems to indicate a considerable degree of local order in samples of this polymer.

2. NMR Polarization Transfer and Local Order

A detailed discussion of the NMR technique employed here is given in ref 8. In this paper, we will limit ourselves to a brief description. 2D polarization-transfer NMR in static solids permits one to monitor the rate of magnetization exchange between two spin packets A and B that have their chemical shielding anisotropy (CSA) tensors differently oriented in the static magnetic field B_0 and, consequently, resonate at different frequencies, Ω_A and Ω_B. The rate constant of polarization transfer is given by[8]

$$R_{AB}(\Omega_A,\Omega_B) = \frac{\pi}{2} s_{AB}{}^2 g_{AB} F_{AB}(0) \qquad (1)$$

g_{AB} is the geometrical rate factor for the spin pairs that resonate at frequencies Ω_A and Ω_B, $F_{AB}(\omega)$ is the corresponding zero-quantum (ZQ) spectrum, and s_{AB} is the dipolar scaling factor. In the rf-driven polarization-transfer technique, a strong radio-frequency field is applied during the polarization-transfer period, for example in the form of a WALTZ17 pulse sequence at a field strength corresponding to 100 kHz. In this situation, $F_{AB}(0)$ and s_{AB} are nearly equal for all ^{13}C-spin pairs in singly ^{13}C-labeled amorphous polymers. This uniformity is the main advantage of the rf-driven technique over other polarization-transfer methods. Numerical and experimental evidence is given in ref 8.

Under ideal conditions, the dipolar scaling factor s_{AB} is $-1/2$ in the presence of the rf field, and we find for an ensemble of N interacting spins[8]

$$g_{AB} = \frac{N}{n_A n_B} \sum_i^{n_A} \sum_j^{n_B} b_{ij}{}^2 = \frac{N}{n_A n_B} \left(\frac{\mu_0}{4\pi} \frac{\hbar\gamma^2}{2} \right)^2 \sum_i^{n_A} \sum_j^{n_B} \left(\frac{1 - 3\cos^2\theta_{ij}}{r_{ij}{}^3} \right)^2 \qquad (2)$$

n_A and n_B are the numbers of spins with frequencies in

[†] Laboratorium für Physikalische Chemie.
[‡] Institut für Polymere.
[§] Present address: The DuPont Co., Central Research and Development, Wilmington, DE 19880.
[||] Present address: Laboratory of Physical Chemistry University of Nijmegen Toernooiveld, 6525 ED Nijmegen, The Netherlands.
[⊗] Abstract published in *Advance ACS Abstracts,* June 15, 1995.

0024-9297/95/2228-5320$09.00/0

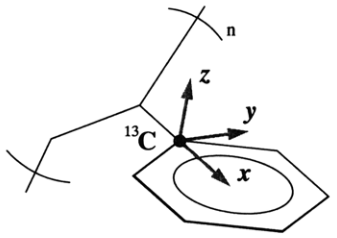

Figure 1. Monomeric unit of polystyrene ^{13}C-labeled at position 1 in the phenyl group. The axis system attached to the labeled carbon indicates the orientation of the chemical shielding anisotropy tensor in the molecular frame. Here, z is the most shielded and x the least shielded axis.

the small resolution intervals $\Omega_A \pm \delta/2$ and $\Omega_B \pm \delta/2$, respectively, and b_{ij} is the dipolar coupling frequency between spin i and spin j. The gyromagnetic ratio is denoted by γ, r_{ij} is the distance between spins i and j, and θ_{ij} is the angle between the internuclear vector and the static magnetic field B_0. In the presence of local order, the geometrical rate factor g_{AB} is correlated with the resonance-frequency pair (Ω_A, Ω_B). Because of the proportionality between $R_{AB}(\Omega_A,\Omega_B)$ and g_{AB}, both quantities can be interpreted in terms of local order. In the following, we will apply this idea to an investigation of local ordering of the phenyl groups in amorphous atactic polystyrene.

The orientation of the phenyl rings is monitored by the chemical shift of the selectively 99% ^{13}C-enriched carbon at ring position 1 (and ^{13}C-depleted at the methylene carbon). Labeled a-PS was produced by free-radical polymerization of [1-^{13}C][β-^{12}C]styrene (^{13}C > 99%, ^{12}C > 99.9%).[8] The polymer is characterized by $M_w = 105\,000$, $M_w/M_n = 1.7$, and $T_g = 95$ °C. The NMR sample was prepared by annealing the labeled polymer at 150 °C for 4 h. The most shielded axis of the CSA tensor of the enriched carbon (z) is, as indicated in Figure 1, perpendicular to the aromatic plane whereas the least shielded axis (x) is aligned with the phenyl bond connecting the side group to the main chain. Small deviations from this orientation could be induced by an asymmetric environment, but according to experience with related compounds[10] they should not exceed 3°.

The 2D spectrum of the labeled polymer with zero mixing time is displayed in Figure 2a. The shape along the diagonal represents the one-dimensional powder pattern. The 2D spectrum of Figure 2b was recorded with a mixing time of 10 s using the proton-driven polarization-transfer technique.[8] During this time, polarization diffuses over 50−80 Å. Since apparently all sections along ω_1 or ω_2 correspond to the one-dimensional powder pattern, the polarization has been redistributed during the mixing time among all possible orientations of the phenyl groups. It demonstrates that no orientational correlation among the side groups extends over more than about 50 Å. This quasi-equilibrium 2D spectrum, however, contains no information on more local order.

Studying local order requires the measurement of polarization-transfer rate constants. Figure 3a shows the rate constants obtained in the initial-rate approximation for the entire cross-peak region of the 2D spectrum of labeled a-PS at 298 K. A series of eight 2D rf-driven polarization-transfer spectra with mixing times from 0.5 to 4 ms were recorded, using the WALTZ17 pulse sequence at a field strength of 100 kHz for the ^{13}C spin locking. The rate constants R_{AB} of Figure 3a were obtained by a linear fit to the mixing-

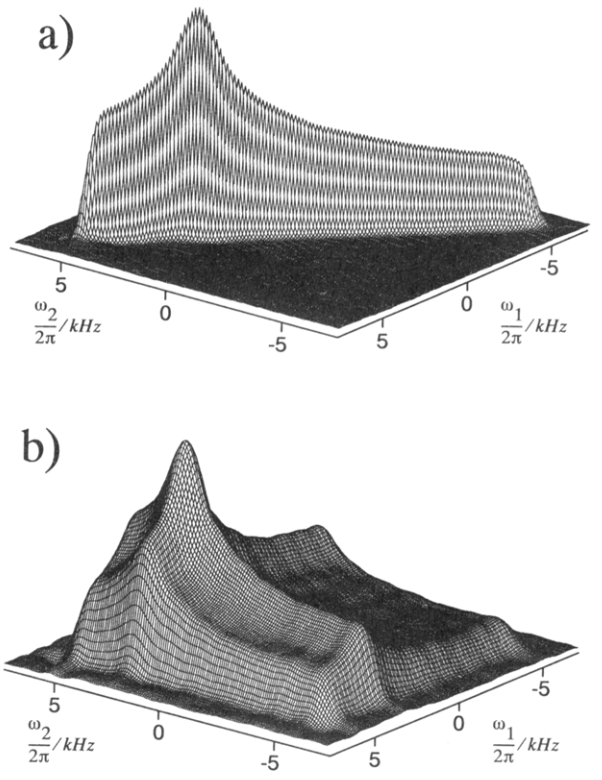

Figure 2. 2D NMR proton-driven ^{13}C-polarization-transfer spectra of singly labeled amorphous a-PS at 295 K (a) with zero mixing time and (b) with a mixing time of 10 s. The spectra were recorded on a home-built spectrometer operating at a proton resonance frequency of 220 MHz. During the mixing time of the 2D experiment, the ^{13}C magnetization is stored along the static magnetic field and no proton decoupling is applied.

time dependence of the intensity at each point in the 2D spectra. Control experiments recorded without rf irradiation during the mixing period exclude any significant contribution from CSA tensor reorientation to the cross-peak intensity.

In the absence of local order among the phenyl rings, all geometrical rate factors g_{AB} are equal and the rate-constant profile should be flat. The deviation from flatness in Figure 3a obviously indicates local orientational correlations among the side chains. The highest rate constants and, thus, the largest mean dipolar couplings are found along the diagonal near the most shielded (low-frequency) region. Neglecting a correlation between the angular term of the dipolar coupling constants ($1-3\cos^2\theta_{ij}$) and the relative orientation of the phenyl groups, these tendencies reveal shorter average distances between rings that are nearly coplanar. They could be the consequence of a specific interaction or caused merely by steric constraints due to the shape of the phenyl rings.

It should be mentioned at this point that the interpretation of the polarization-transfer rate constant $R_{AB}(\Omega_A,\Omega_B)$ in terms of the distances r_{ij} only is incomplete. According to eq 2, there is also a strong orientation dependence introduced by ($1-3\cos^2\theta_{ij}$). A reliable interpretation requires detailed model calculations, including this angular dependence. In contrast to earlier work on local order in polymers[1,2] where RIS models are used to fit the experimental scattering data, we compare the experimental profile of rate constants to a profile computed from atomistic simulations of the bulk amorphous polystyrene structure.[9]

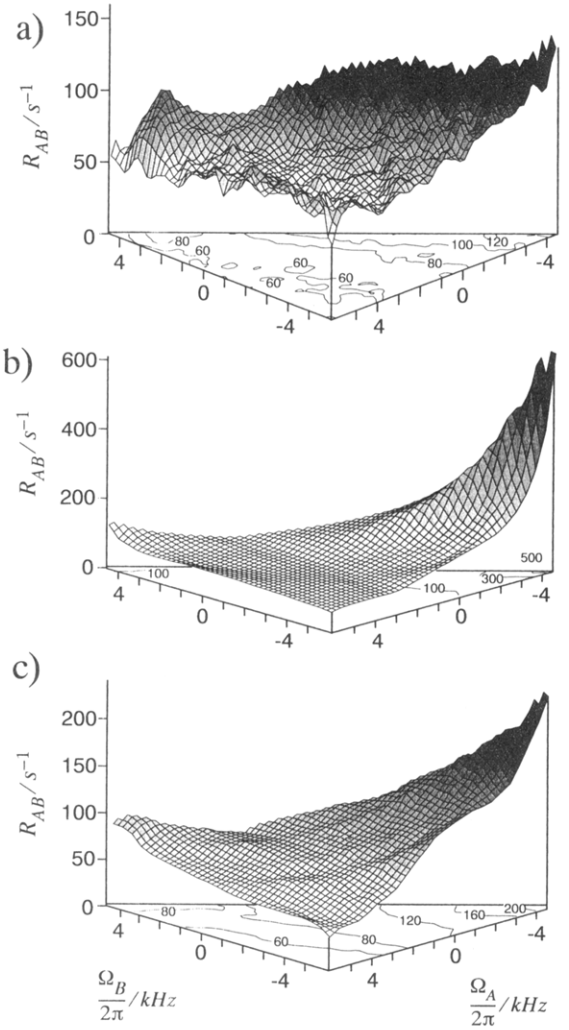

Figure 3. (a) rf-driven polarization-transfer rate constant R_{AB} between isochromates resonating at frequencies Ω_A and Ω_B. The rate constants were obtained from a series of 2D experiments with mixing times up to 4 ms recorded at 295 K and evaluated in the initial-rate approximation. The data were acquired with the spectrometer mentioned in Figure 2. During the mixing time, the ^{13}C magnetization is spin-locked in the transversal plane by a WALTZ17 pulse sequence. The duration of the 17th pulse corresponds to a flip angle of $\pi/2$. Homonuclear BLEW12 proton decoupling is applied simultaneously to the WALTZ17 pulse train. The rf-field strength was set to 100 kHz on both channels. (b) Polarization-transfer rate constants computed from the atomistic simulations as described in the text. The rate constants are averages over 24 independent simulations of a-PS. (c) Polarization-transfer rate constants computed from the simulation showing the best agreement with the experimental values displayed in (a). The rate constants were averaged over 15 structures sampled each picosecond in a 15 ps MD run of the corresponding a-PS simulation at 300 K.

3. Detailed Atomistic Models of Atactic Polystyrene

The computational model consists of 24 sample structures of atactic polystyrene that have been derived from those created by Rapold et al. in ref 9. Each of them is a periodically repeated box of edge length 18.65 Å that contains an atactic chain of 40 monomer units. Because carbon−carbon distances below 3 Å with correspondingly high van der Waals energies appear in the structures of ref 9, the chain packings have been allowed to relax using 25 ps molecular-dynamics (MD) runs flanked by two energy minimizations, each with 500 conjugate-gradient steps. The structure refinements

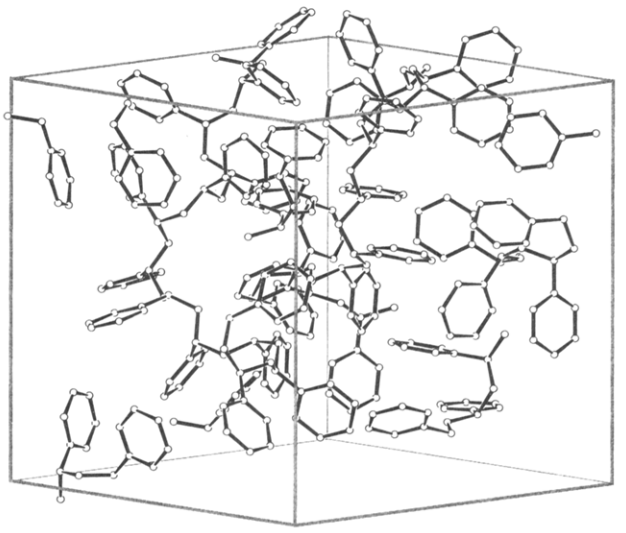

Figure 4. Microstructure of a-PS. The box conforms to periodic continuation conditions and contains 40 monomeric units. Its edge length is 18.65 Å. Only the carbons are represented.

were performed with the Discover program (Biosym Technologies[11]) at constant number of atoms, volume, and temperature (*NVT*). The time increment for the MD runs was 1 fs. In contrast to the force field with fixed bond angles and bond lengths used in ref 9, the unconstrained Cartesian-coordinate force field pcff91[12] was applied. A representative structure is shown in Figure 4 (hydrogen atoms are omitted for clarity).

To gain insight into the local order among the phenyl groups, the distribution of the angle β between phenyl planes was computed for different intervals of distances between labeled sites in pairs of rings. The weighted distribution $p(\beta)/\sin(\beta)$ (Figure 5) shows that for internuclear distances shorter than 5 Å, small angles between the phenyl planes are preferred. Within the statistical error, a flat profile is obtained already for internuclear distances between 5 and 6 Å. Such a profile corresponds to a random angular distribution between the phenyl planes. Also included in the figures are numbers that indicate the fractional contributions of the pairs of nuclei, from which the corresponding histogram was computed, to the sum in eq 2 averaged over all frequencies Ω_A and Ω_B. These numbers give the relative importance of the corresponding distribution for comparison to the NMR data. Obviously, as the distance between the phenyl rings increases, their contribution to the overall result diminishes; nevertheless, the sum of all distances >5 Å constitutes about one-quarter of the total sum and hence has still a significant impact on the interpretation of the experimental results.

4. Comparison between the NMR Results and the Atomistic Simulations

From the phenyl-group positions in the 24 sample structures, the polarization-transfer rate constants have been computed for each frequency pair according to eqs 1 and 2. The principal components of the CSA tensor for computing the resonance frequencies were obtained by a fit to the spectrum presented in Figure 2a (ν_{XX} = 6040 Hz, ν_{YY} = 3290 Hz, and ν_{ZZ} = −6040 Hz, or δ_{XX} = 236 ppm, δ_{YY} = 184 ppm, and δ_{ZZ} = 18 ppm from TMS). The intensity of the ZQ spectrum $F_{AB}(\omega)$ was approximated by convoluting two single-quantum line

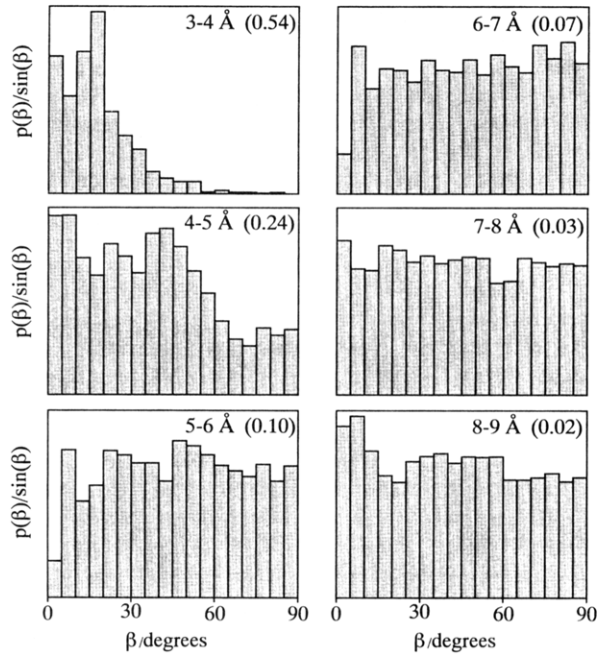

Figure 5. Histograms of the weighted distribution $p(\beta)/\sin(\beta)$ of the angle β between two phenyl planes as a function of the distance between the two carbons at position 1 in the phenyl rings. Each histogram corresponds to pairs of rings that have their labeled nuclei (1-C) at a separation in the indicated interval. The distributions were calculated from the 24 simulations used to compute the data of Figure 3b. The numbers in parentheses are the fractional contributions of the pairs of nuclei, from which the corresponding histogram was computed, to the sum in eq 2 averaged over all frequencies Ω_A and Ω_B. The fractions refer to the pairs distant by less than 9 Å.

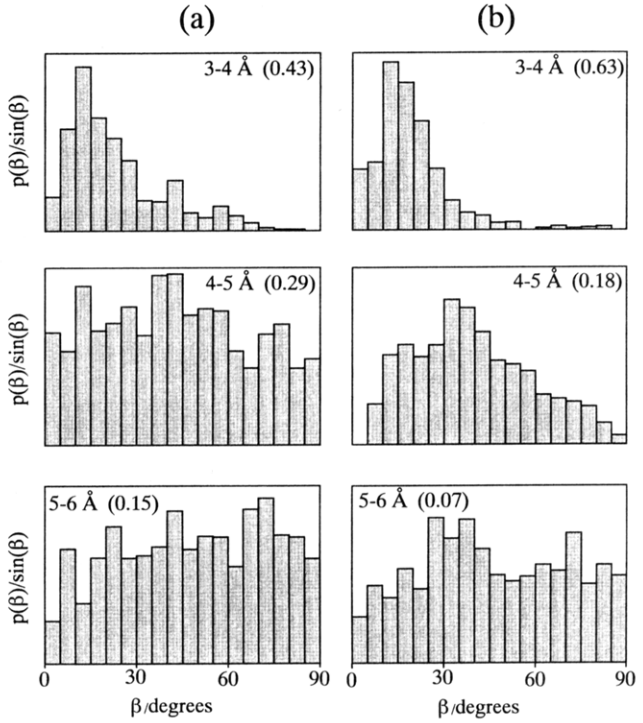

Figure 6. Histograms of the weighted distribution $p(\beta)/\sin(\beta)$ of the angle β between two phenyl planes as a function of the distance between the two carbons at position 1 in the phenyl rings. The distance intervals are given in the figure. The distributions are displayed for two structures out of the 24 and were averaged over 15 time frames sampled each picosecond during a 15 ps MD run at 300 K. The numbers in parentheses are the fractional contributions of the pairs of nuclei, from which the corresponding histogram was computed, to the sum in eq 2 averaged over all frequencies Ω_A and Ω_B. The fractions refer to the pairs distant by less than 9 Å. Column a gives the distributions for the structure whose rate constants best agree with the experimental ones. Column b shows the distributions for the structure whose rate constants give the worst agreement with the experimental ones.

shapes[8] taken perpendicular to the diagonal of the spectrum of Figure 2a. Taking into account the scaling of the dipolar interactions by a factor $-1/2$, $F_{AB}(0)$ was found to be approximately 8.4×10^{-4} s. This evaluation leads to a slightly underestimated value because it does not exclude the line width contribution of the pairs that resonate at frequencies Ω_A and Ω_B.

Of special concern is the question of finite-size effects, i.e., the limitations of the computational accuracy due to the finite box size of the atomistic simulations. The number of pairs (A, B) at a given distance r grows approximately with r^2; their individual contribution to g_{AB} is proportional to r^{-6}. Thus, the contributions to eq 2 decrease as r^{-4} for large distances. The maximum distance between two nuclei that are not correlated spatially through the continuation conditions of the microstructures is half the edge size, i.e., ca. 9 Å. Since the distance between neighboring labeled carbons is less than 5 Å, the convergence of the sum in eq 2 is ensured with sufficient accuracy as suggested by the fractional contributions of the different distance intervals in Figure 5.

The computed rate constants are plotted in Figure 3b; they show qualitatively the same tendencies as the experimental data of Figure 3a: higher rate constants along the diagonal and on the side of the most shielded (low-frequency) region. However, the variation within the computed profile is larger by a factor of 4. Figure 3c shows the rate constant profile for the computed structure out of the 24 that agrees best with the experimental results. Here, 15 time frames sampled each picosecond during a 15 ps MD were used to compute an average profile. The differences between this profile and the one of Figure 3b characterize the typical deviations among the 24 boxes. The distribution $p(\beta)/\sin(\beta)$ computed from the 15 time frames is displayed in Figure 6a. Figure 6b shows the corresponding distribution obtained from the structure whose rate constants exhibit the worst agreement with the experimental data. None of the distributions reveal significant correlation among the orientations of phenyl planes with distances beyond 5 Å. A comparison of parts a and c of Figure 3 shows that the local order sensed by the NMR polarization-transfer experiments is even weaker than in the most disordered structure (Figure 6a). Thus, orientational correlation among the phenyl groups in polystyrene is limited to less than 5 Å and might be merely determined by the geometrically restricted proximity for rings with large angles ($\beta \rightarrow 90°$) between their planes.

The steady increase of the computed rate constants along the diagonal of Figure 3b,c from its minimum value toward the least shielded (high-frequency) region indicates that in addition to coplanarity of the rings also colinearity is favored. In contrast, the experimental data of Figure 3a display a more complex behavior parallel to the diagonal. In addition to the trends seen in the computed profiles of Figures 3b,c, there is a local peak at $\Omega_A/2\pi \cong 4.4$ kHz and $\Omega_B/2\pi \cong 3.3$ kHz between the two least shielded principal components of the CSA tensor. Its explanation requires the abundance of spatially near rings that are not simultaneously copla-

nar and colinear. Such findings might help to refine the potentials in the atomistic simulations or the method used for folding and packing the polymer chains.[9]

5. Comparison with Other Measurements and Conclusions

Previous investigations of local order in atactic polystyrene by wide-angle X-ray scattering[1] and by wide-angle neutron scattering[3,4] had led to the postulate of pronounced ordering in a-PS glasses. In the X-ray study, a supermolecular structure was proposed with stacking of the phenyl rings and ordering over distances up to 15 Å within and between adjacent stacks. The neutron diffraction data were interpreted in terms of paracrystallites with a grain size of 20 Å. The results presented here contrast markedly with these findings. The NMR data agree well with molecular models where orientational correlations among the phenyl planes do not extend over more than 5 Å. They support the concept of randomly coiled chains with large variations of the diad conformations, as discussed in ref 9.

NMR is by nature a technique very sensitive to local structural features because the involved nuclei are acting as localized reporters that can be addressed individually provided that their orientation-dependent chemical shifts are sufficiently distinct. It has thus a specificity hardly matched by any other techniques. Especially when combined with site-selective isotopic labeling, it presents itself from its best side.

NMR polarization-transfer experiments provide two types of information that are relatively easy to interpret. Two-dimensional polarization-transfer spectra with an extended transfer time, approaching a quasi-equilibrium state, such as the spectrum of Figure 2b, measure the presence or absence of long-range order over 50–100 Å. On the other hand, the polarization-transfer rate constants, measured in the initial-rate regime, monitor short-range order up to 5–10 Å. The intermediate distance range can, in principle, be studied by polarization-transfer experiments with intermediate transfer times. Multiple transfer steps occur under these conditions, and the analysis requires a full dynamic simulation of the polarization-transfer network based on a detailed atomistic model of sufficient spatial range (≈50 Å). Reliable atomistic models of this size are not yet available. Therefore, we have compared in the present paper the results of small-scale atomistic modeling with the short-range order manifested in the initial-rate regime. The conclusions about the absence of ordering extending to 10–20 Å are thus based on an extrapolation from the atomistic model calculations assuming that the orientational correlation among the phenyl rings decays with increasing ring distances.

So far the effects of molecular mobility have not been mentioned. X-ray and neutron scattering correlate instantaneous orientations, and molecular motion leads to a broadening of the observed angular distribution function. On the other hand, the NMR observation inherently involves an averaging process over a time of a few 100 μs. Thus, motionally averaged structures are correlated in polarization-transfer experiments, and NMR should in fact observe more local order than either X-ray or neutron diffraction. This further increases the discrepancy between scattering and NMR results on amorphous atactic polystyrene.

In summary, the NMR polarization-transfer results reported here can be explained fully by orientational correlation between rings in very close spatial proximity (their carbon atoms in the 1-position being separated by less than 5 Å) and essentially no correlation between rings further apart (separation larger than 5 Å). At distances of approximately 50 Å, the mutual orientation of phenyl rings is experimentally clearly random. However, a specific intermediate-range order appearing in a window of, e.g., 15–30 Å cannot be ruled out, although it is difficult to imagine what the driving force of such an ordering would be.

Acknowledgment. We are indebted to Dr. Roland Rapold and Marcel Zehnder for their help with the molecular modeling. This work has been supported by the Swiss National Science Foundation and by the Aluminium Fonds, Neuhausen.

References and Notes

(1) Mitchell, G. R.; Windle, A. H. *Polymer* **1984**, *25*, 906–920.
(2) Mitchell, G. R. *Comprehensive Polymer Science*; Pergamon: Oxford, U.K., 1989; Vol. 1, pp 687–729.
(3) Schärpf, O.; Gabrys, B.; Pfeiffer, D. G. *ILL Report No. 90SC26T*; Grenoble, 1989.
(4) Gabrys, B.; Schärpf, O.; Pfeiffer, D. G. *J. Polym. Sci.* **1993**, *B31*, 1891–1895.
(5) Born, R.; Spiess, H. W.; Kutzelnigg, W.; Fleischer, U.; Schindler, M. *Macromolecules* **1994**, *27*, 1500–1504.
(6) Robyr, P.; Meier, B. H.; Ernst, R. R. *Chem. Phys. Lett.* **1989**, *162*, 417–423.
(7) Meier, B. H. *Adv. Magn. Opt. Reson.* **1994**, *18*, 1–116.
(8) Robyr, P.; Tomaselli, M.; Straka, J.; Grob-Pisano, C.; Suter, U. W.; Meier, B. H.; Ernst, R. R. *Mol. Phys.* **1995**, *84*, 995–1020.
(9) Rapold, R. F.; Suter, U. W.; Theodorou, D. N. *Macromol. Theory Simul.* **1994**, *3*, 19–43.
(10) Veeman, W. S. *Prog. Nucl. Magn. Reson. Spectrosc.* **1984**, *16*, 193–235.
(11) Discover3.1 and InsightII. Biosym Technologies, Inc., San Diego, CA, 1993.
(12) Maple, J. R.; Hwang, M.-J.; Stockfisch, T. P.; Dinur, U.; Waldman, M.; Ewig, C. S.; Hagler, A. T. *J. Comput. Chem.* **1994**, *15*, 162–182.

MA950106S